Research Open

Geology, Earth and Marine Sciences

Volume 8 Issue 6

Research Article

Direct Mantle–Crust Interaction by Supercritical Fluids and Melts: Evidence from High-Pressure Mineral Inclusions

Thomas R[1] and Pei Ni[2]

Im Waldwinkel 8, D-14662 Friesack, Germany

[2]Nanjing University, China

***Corresponding author:** Rainer Thomas, D-14662 Friesack, Germany

Received: July 02, 2026; **Accepted:** July 06, 2026; **Published:** July 09, 2026

Abstract

High-pressure and ultra-high-pressure mineral inclusions enclosed in comparatively low-pressure crustal rocks provide evidence for rapid material transfer between deep lithospheric or mantle-related domains and upper-crustal mineral-forming environments. This study summarizes observations from emerald-bearing rocks of the Habachtal/Austria, prismatine granulite from Waldheim/Saxony, topaz from the Greifenstein granite, cassiterite from Variscan tin deposits, and related occurrences. The documented phases include diamond, moissanite, coesite, stishovite, lonsdaleite, reidite, orthorhombic cassiterite, and other high-pressure minerals. Many occur as smooth spherical or subspherical crystals, locally with composite textures, indicating entrainment, mechanical abrasion, and possible chemical modification during transport. These features cannot be explained satisfactorily by conventional low-pressure hydrothermal models or by equilibrium mineral assemblages inferred for the host rocks. Instead, they are interpreted as evidence for transfer by supercritical fluids or melts in which H_2O and aluminosilicate components are fully miscible. Such media combine high mobility with the capacity to carry dissolved elements and suspended mineral relics, allowing tiny high-pressure crystals to move rapidly through the crust and survive before complete inversion to low-pressure polymorphs. The Raman-confirmed presence of diamond spherules in emerald from Habachtal provides additional evidence that high-pressure mineral relics were transported into the emerald-forming environment by supercritical media. These supercritical systems also provide a mechanism for extreme, selective enrichment of elements. Water-rich melt inclusions, Lorentzian element distributions, and high Sn and Be concentrations indicate non-equilibrium concentration during the transition from supercritical to undercritical conditions. Together, the evidence supports direct mantle–crust interaction mediated by supercritical fluids or melts and suggests that this process may be important, but previously underestimated, in the formation of granitic, pegmatitic, and ore-related systems..

***Keywords:** Coesite, Diamond, High-pressure mineral inclusions, Mantle–crust interaction, Metal enrichment, Moissanite, Supercritical fluids, Supercritical melts, Trans-crustal transport, Water-rich melt inclusions.*

Introduction

High-pressure and ultra-high-pressure mineral inclusions hosted by rocks that otherwise record comparatively low-pressure crustal conditions pose a fundamental problem for conventional models of crustal mineral formation. Minerals such as diamond, moissanite, coesite, stishovite, reidite, lonsdaleite, and orthorhombic cassiterite require formation or stabilization at pressures far above those inferred for many host assemblages. Their survival in granitic, pegmatitic, metamorphic, and ore-related settings therefore requires a mechanism capable of rapidly transferring material from deep lithospheric or mantle-related domains into upper-crustal environments while limiting transformation to lower-pressure polymorphs. Recent observations from emerald-bearing rocks of the Habachtal, prismatine-bearing granulite from Waldheim in the Saxon Granulite Massif, topaz from the Greifenstein granite, and cassiterite from Variscan tin deposits point to such a process. These occurrences contain high-pressure mineral relics, water-rich melt inclusions, and trace-element distributions that are difficult to explain by equilibrium crystallization or conventional low-temperature hydrothermal redistribution alone. In several examples, the inclusions are smooth, spherical to subspherical, or composite, suggesting entrainment, mechanical abrasion, and possible chemical modification during ascent. This contribution evaluates the interpretation that supercritical fluids or melts served as the principal carrier. When H_2O and aluminosilicate components become fully miscible, supercritical media can combine the mobility of fluids with the element-carrying capacity of melts. In this state, they can mobilize dissolved components and entrain mineral relics, enabling rapid trans-crustal transfer of high-pressure phases and selective enrichment of metals and volatile components. The paper builds on earlier work presented at the ACROFI IX meeting in Nanjing in 2022, where complete miscibility between silicate melts and hydrous fluids and the enrichment of selected elements in the supercritical state were discussed. Since then, additional observations have strengthened the case that this mode of transfer may represent a broader geological process. The following sections summarize key examples and examine their implications for direct mantle–crust interaction, rapid material movement, and the formation of granitic, pegmatitic, and ore-related systems.

Results

Emerald from the Habachtal

The Habachtal emerald deposit provides an important starting point for evaluating the role of deep-derived inputs in crustal mineral-forming systems [1,2]. Re-homogenization experiments on melt inclusions yielded temperatures of approximately 700°C at 5 kbar, substantially higher than many earlier estimates for emerald formation in this locality. As shown in Figure 1, a key observation is the presence of water-rich melt inclusions containing approximately 30 wt.% H_2O. These inclusions were previously easy to overlook or misclassify as solid inclusions, but their abundance and composition indicate that they are central to understanding emerald formation at Habachtal. Similar secondary inclusion planes have also been observed in topaz from Schneckenstein [3], where they occur perpendicular to the c-axis. Following Taleb's (2018) [4] emphasis on rare but highly significant observations, these inclusions can be regarded as diagnostic rather than incidental. Their occurrence challenges interpretations based solely on conventional fluid inclusions. In addition, Figure 2 shows a well-defined Lorentzian relationship between $MgCO_3$ content and water concentration, suggesting non-equilibrium enrichment in a supercritical medium.

The relationship shown in Figure 2 can be interpreted as evidence for an ion-exchange process involving carbonate complexes, expressed schematically as $BeCO_3 \rightarrow MgCO_3$. In this interpretation, Be was transported in a supercritical fluid as a carbonate species, whereas Mg was supplied by interaction with the surrounding rocks. A broader summary of supercritical fluids and melts in granites and pegmatites is given by Thomas et al. (2022) [5].

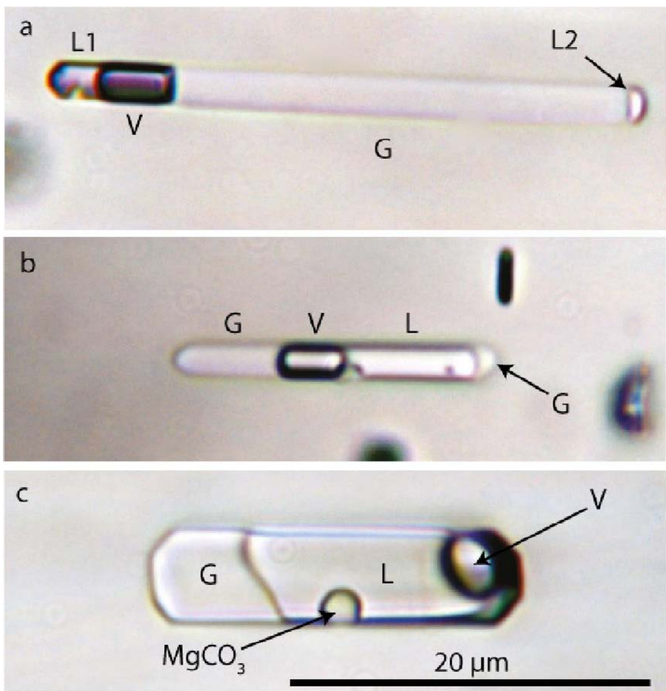

Figure 1: Melt inclusions in emerald from Habachtal/Austria. a) Melt inclusion in emerald composed of a large glass part (G), two liquid phases L1 and L2, and a small vapor phase (V). b) Melt inclusion in emerald with glass (G), liquid (L), and vapor (V). c) Melt inclusion in the same emerald crystal. G – glass, L - liquid phase, V -vapor phase, and a $MgCO_3$ daughter crystal.

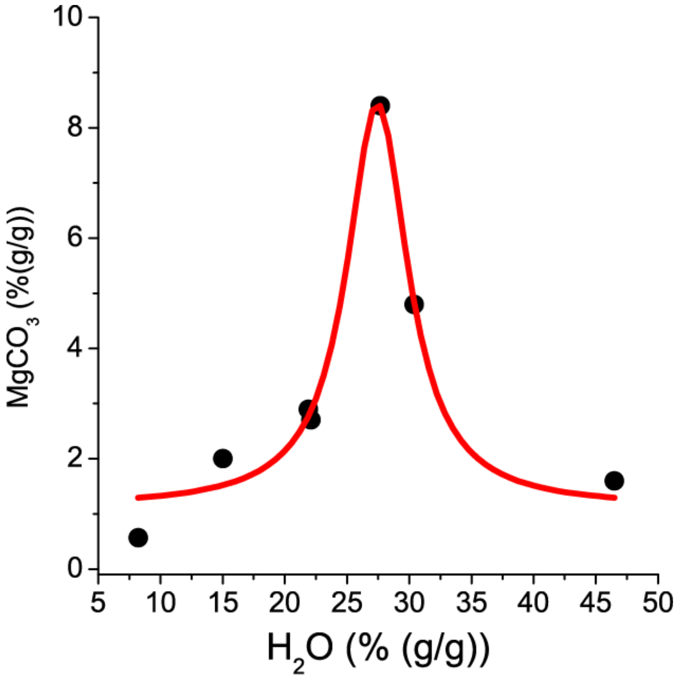

Figure 2: Lorentzian distribution of $MgCO_3$ content versus water concentration in carbonate-bearing melt inclusions.

Table 1: Results of Raman measurements in the first-order diamond Raman region of emerald from Habachtal, Austria.

Diamond	FWHM	G-band	FWHM	n
1331.5 ± 1.5 cm^{-1}	62.0 ± 20.0 cm^{-1}	1579.1 ± 6.4 cm^{-1}	63.2 ± 12.4 cm^{-1}	9

FWHM = full width at half maximum; n = number of measured crystals.

New Raman spectroscopic results, including the detection of diamond spherules in emerald and in melt inclusions, support the involvement of supercritical media in emerald formation (Table 1).

The broad first-order diamond band and associated G-band indicate very small, structurally imperfect diamond or diamond-like carbon (DLC) particles, consistent with rapid transport and partial modification in a supercritical medium. The principal result from Habachtal is that emerald crystallization began near 700°C and 5 kbar from a supercritical, water-rich silicate melt containing approximately 30 wt.% H_2O. These conditions require a reassessment of the deposit's formation model. These results contrast with previously accepted pressure-temperature estimates for the pre-Alpine event (<3 kbar and <450°C) and the Alpine event (4.5–6 kbar and 500–550°C [6-9]. Those estimates were derived mainly from mineral equilibria, whereas the present observations point to a supercritical input that may not have been in equilibrium with the host assemblage.

Spherical Crystals in the Prismatine Rock from Waldheim/Saxony

To test whether this process is restricted to Habachtal or reflects a broader phenomenon, prismatine-bearing granulite from Waldheim in the Saxon Granulite Massif was examined by polarization microscopy and micro-Raman spectroscopy. The Waldheim samples contain ultra-high-pressure mineral inclusions in rocks that otherwise record crustal metamorphic conditions. Water-rich stishovite and coesite occur in the prismatine-bearing granulite. According to Ono et al. (2017) [9], these phases indicate pressures of approximately 8–9 GPa at about 1000°C, corresponding to depths of roughly 240–300 km. These values are far higher than the maximum pressure of about 1.0 GPa estimated for prismatine crystallization by Rötzler et al. (2008) [10]. A characteristic feature of the Waldheim material is the abundance of spherical to subspherical mineral inclusions with smooth surfaces and diameters commonly between 10 and 50 µm. These inclusions are mostly monomineralic and include zircon, diamond, moissanite, coesite, and related phases. They occur mainly in prismatine but are also present in corundum, dravite, garnet, and sillimanite. In the prismatine rock, the zircon sphere frequency is approximately 180 per cm^3. Kalkowsky (1907) [11] had already described such smooth zircon spheres as resembling oil drops, although no genetic interpretation was proposed at that time. Some inclusions are composite, with one rounded crystal enclosed within another; for example, anorthite spheres occur within a corundum matrix. These textures suggest mechanical abrasion and possible chemical corrosion during movement in a fast-moving supercritical fluid or melt. The occurrence of spheres within spheres further implies that the process was multi-stage. Figures 3–6 illustrate representative spherical and subspherical inclusions from the Saxon Granulite

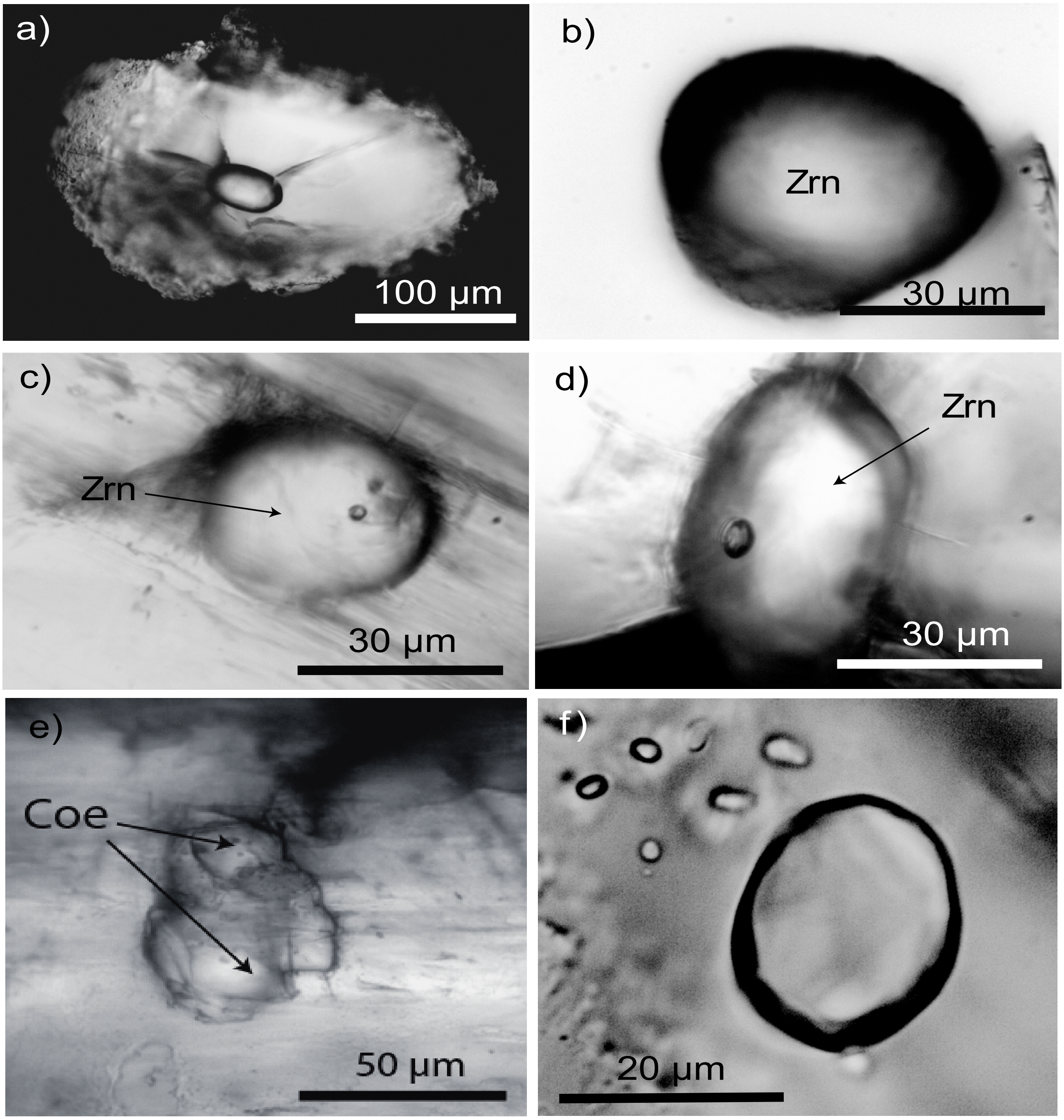

Figure 3: a) Reidite-zircon inclusion in quartz. b to d) zircon in prismatine. e) a conglomerate of coesite ellipsoids in prismatine. f) spherical anorthite crystals in an ellipsoid corundum crystal.

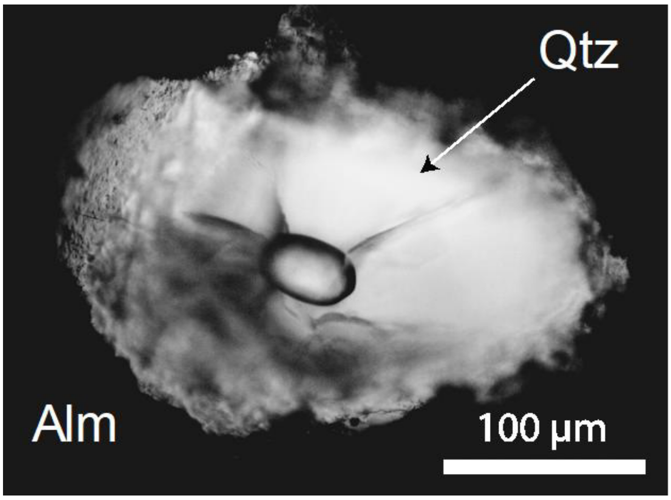

Figure 4: Zircon-reidite crystal in the center of a high-quartz crystal.

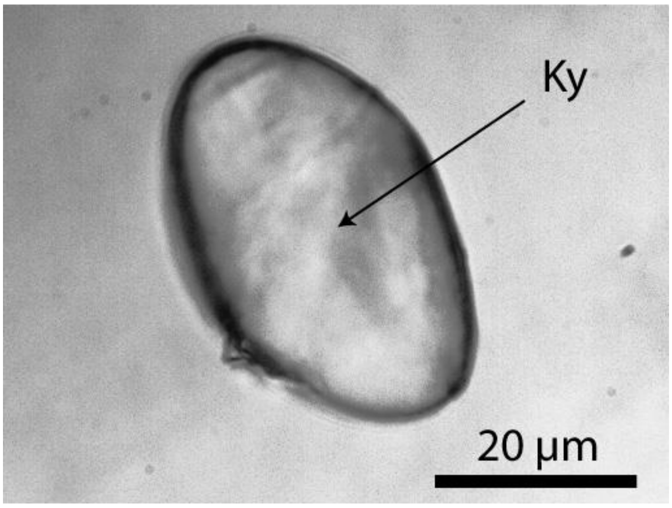

Figure 5: Elliptical kyanite inclusion in dravite. Near this inclusion is a spherical aggregate of nano-diamond, moissanite, and graphite, as well as a water-rich supercritical melt inclusion.

Massif. Their morphology and internal relationships provide direct textural evidence for transport and entrainment.

Figure 4 shows a zircon–reidite inclusion in the center of an elliptical high-quartz crystal. Radial fractures in the quartz host are consistent with volume expansion during the transformation of primary reidite to zircon. Figure 5 shows an elliptical kyanite inclusion in dravite.

The zircon–reidite transition requires minimum pressures of approximately 8–12 GPa at 1100–1900 K under supercritical conditions [12].

Figure 6 shows albite enclosed within a spherical corundum crystal, providing another example of a composite inclusion texture. These spherical crystals are mineralogically foreign to the Waldheim prismatine assemblage and are therefore interpreted as exotic inclusions introduced during rapid transport via supercritical media.

If supercritical transfer is a general geological process, comparable evidence should occur in other settings. Variscan mineralizations in the Erzgebirge commonly show features consistent with supercritical fluids or melts. That prompted a search for comparable rounded inclusions in granitic minerals, where similar textures were identified in topaz and plagioclase.

Spherical Crystals in Topaz from the Greifenstein Granite

Topaz from the Greifenstein granite contains numerous rounded to elliptical inclusions. Their smooth morphology suggests incorporation during the rapid crystallization of the host topaz. Such rapid growth may have helped preserve high-pressure minerals derived from greater depth (Figure 7).

As in the Waldheim prismatine rock, the Greifenstein inclusions are out of equilibrium with the low-pressure host assemblage. Their occurrence in topaz therefore provides additional evidence for the introduction of high-pressure and high-temperature mineral relics from deeper domains (Figures 8-10).

Note that the SiC powder used for sample preparation has a grain size of 10 μm and always shows sharp edges (Figure 11).

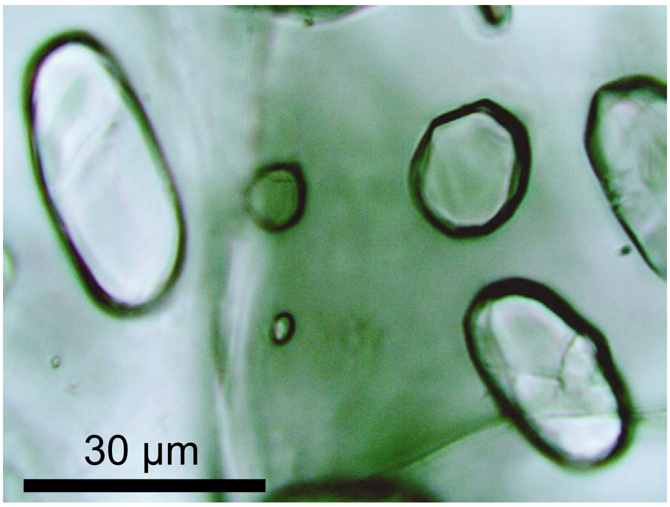

Figure 6: Albite inclusion in a spherical corundum crystal.

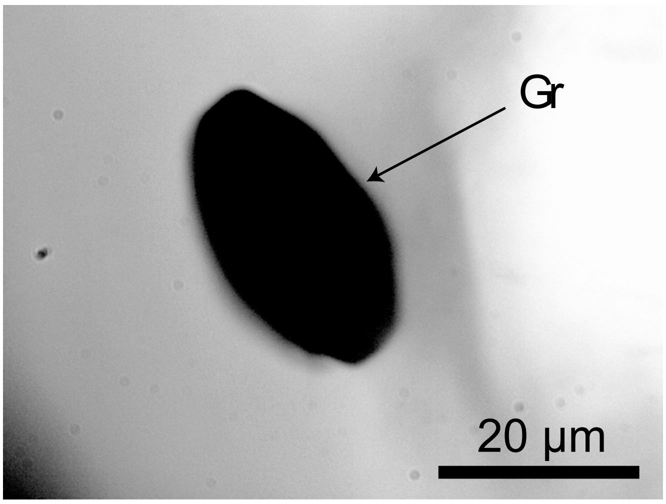

Figure 7: Disk-like elliptical graphite inclusion in topaz of the Greifenstein granite.

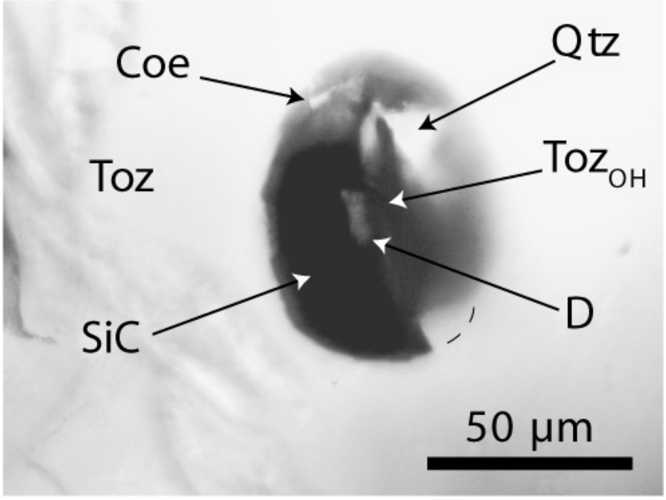

Figure 8: Diamond in a moissanite (SiC)-rich spherical inclusion in topaz from the Greifenstein granite. This inclusion is about 30-55 µm below the surface of the 300 µm-thick sample. Toz – topaz host crystal, Toz_{OH} – OH-rich topaz, SiC – moissanite, D – diamond, Qtz – quartz (primary stishovite or coesite - see the asymmetric volume change), Coe – coesite.

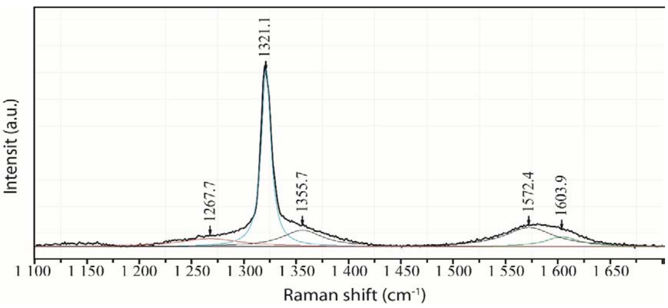

Figure 9: The diamonds in moissanite in topaz of the Greifenstein granite are mainly of the hexagonal diamond polytype. From 28 measurements, we obtained a value of 1325.4 ± 4.4 cm^{-1} for the diamond first-order line. The FWHM is 10.8 ± 4.1 cm^{-1}. FWHM - Full Width at Half Maximum.

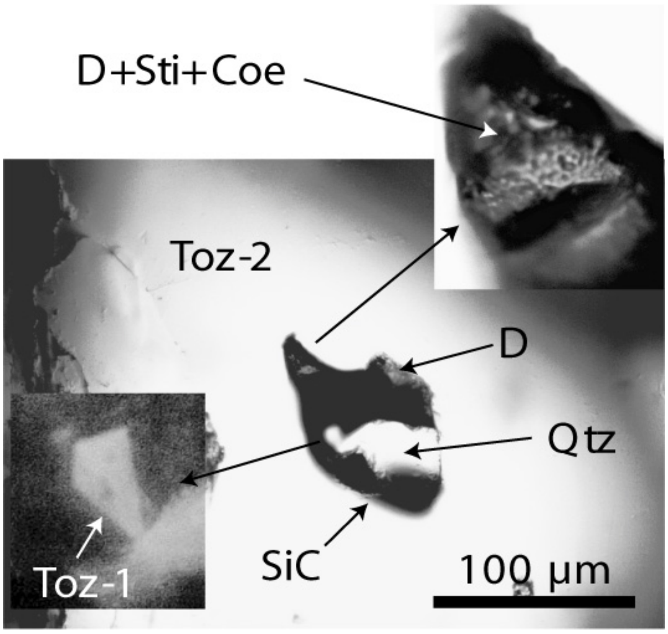

Figure 10: A complex moissanite (SiC) inclusion in topaz (Toz-2) from the Greifenstein. granite. D – diamond, Sti – stishovite, Coe - coesite, Qtz – quartz. Toz-1 is an earlier topaz inside the moissanite aggregate. The paragenesis clearly shows that no preparation step introduces the moissanite inclusion.

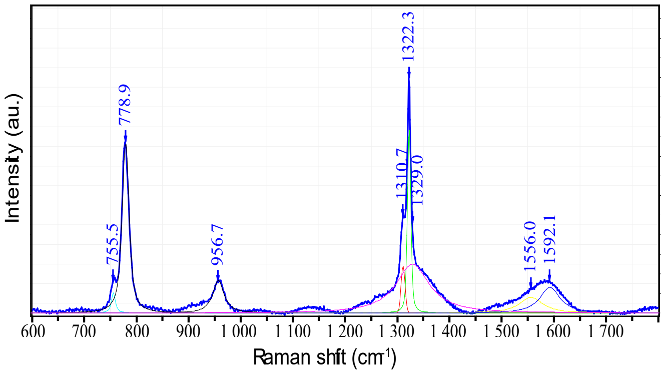

Figure 11: Raman spectrum of moissanite, with bands at 755.5, 778.9, and 956.7 cm^{-1}, and a two-phase diamond–lonsdaleite particle, with bands at 1310.7 and 1322.3 cm^{-1}. The lonsdaleite mode of hexagonal diamond can vary between 1320 and 1327 cm^{-1}.

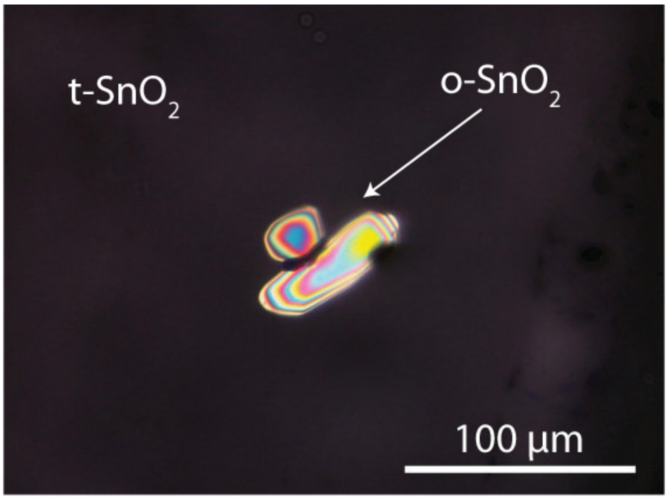

Figure 12: Orthorhombic cassiterite (o-SnO_2) in tetragonal cassiterite (t-SnO_2) Sn-19 from the Sauberg mine near Ehrenfriedersdorf.

Additional evidence comes from ore minerals that contain relics of high-pressure, high-temperature conditions. A representative example is the occurrence of mostly rounded orthorhombic cassiterite inclusions in tetragonal cassiterite from Variscan tin deposits in the Erzgebirge and Slavkovský les [11,12]. Figure 12 illustrates orthorhombic cassiterite inclusions in tetragonal cassiterite.

Orthorhombic cassiterite inclusions in tetragonal cassiterite are abundant in several samples. For example, the cassiterite sample Sn-58 from Ehrenfriedersdorf contains more than 120,000 orthorhombic cassiterite crystals per cm^3, with a mean diameter of 13.2 µm. Larger grains also occur; in sample Sn-70, grains reach 320 µm in diameter. Many orthorhombic cassiterite crystals are of the $CaCl_2$-type structure and correspond to pressures of approximately 18.9 GPa [14], and references therein. Also, the cotunnite-type ($PbCl_2$-type), which forms at pressures >74 GPa and high temperatures, is not rare. Their abundance suggests that Sn was not derived solely from the surrounding granite, but was introduced at least in part by supercritical fluids or melts from greater depth. A simple mass-balance calculation [13] supports this conclusion, because the approximately 38 ppm Sn content of the surrounding granite is insufficient to generate such a large and rich tin deposit. Earlier genetic models explained Variscan tin mineralization mainly through redistribution of granite-derived Sn by

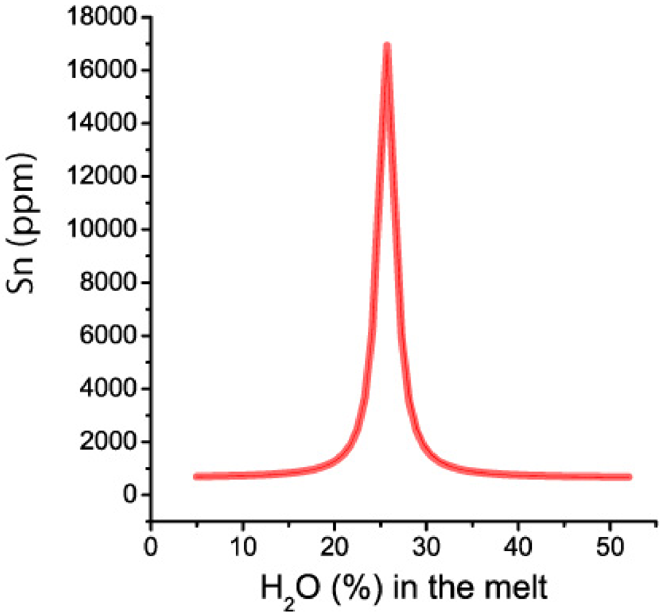

Figure 13: Ehrenfriedersdorf, Sauberg mine: Lorentzian distribution of tin versus water concentration of the corresponding solvus curve. The maximum is about 16,300 ppm Sn and corresponds to the maximum solubility of Sn at the transition from supercritical to undercritical conditions at about 750°C.

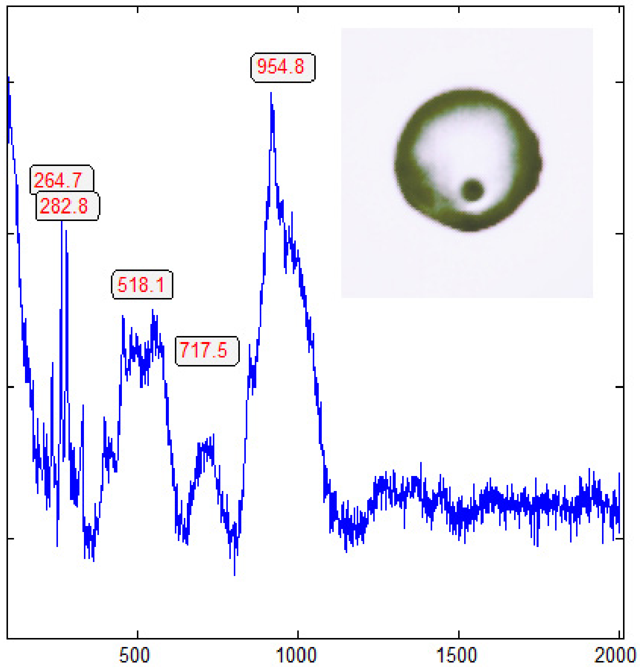

Figure 14: Raman spectrum of a mixture of a- and b-rhombohedral boron in topaz from Schneckenstein. The inset shows a spherical boron crystal with a diameter of 9 µm at a depth of 10 µm. The dark inclusion, possibly diamond, shows that the boron is transparent.

low-temperature hydrothermal processes, supported by fluid-inclusion homogenization temperatures near 400°C. However, the discovery of melt inclusions in quartz containing up to 16,300 ppm Sn substantially changes this interpretation. As in the Habachtal emerald system, conventional fluid inclusions appear to record secondary or late-stage processes rather than the primary metal-transport event (Figure 13).

Similar Lorentzian distributions, expressed as element concentration versus melt inclusion water content, were observed for 20 elements [5]. We interpret these distributions as resulting from direct interaction between supercritical fluids and/or supercritical melts generated in mantle regions and the crust. A further example is provided by topaz from Schneckenstein [3]. This topaz contains numerous fluid inclusions on planes perpendicular to the c-axis, with homogenization temperatures of 407 ± 25°C. Although these inclusions may appear primary, the same topaz also contains remnants of high-temperature, high-pressure Ti-topaz, diamond-like carbon (DLC) spheres, and statistically distributed spherical, colorless boron inclusions. Boron is normally black or dark-coloured and opaque, but it can become transparent under high pressures of approximately 19–89 GPa as boron atoms rearrange into different crystal structures [16]. Figure 14 shows a Raman spectrum of a mixture of α- and β-boron, as well as a photomicrograph of such a transparent boron sphere.

The Raman bands around 265 and 283 cm^{-1} are due to the topaz matrix. Because of the large Al supply from the topaz matrix, α- and β-AlB_{12} components are possible [3,17].

Conclusion

The results show that minerals preserved in comparatively low-pressure crustal host rocks contain inclusions that require high-pressure to ultra-high-pressure conditions. These phases include diamond, boron, moissanite, coesite, stishovite, lonsdaleite, reidite, orthorhombic cassiterite, and related minerals. Their occurrence in emerald, prismatine granulite, topaz, and cassiterite is difficult to reconcile with conventional equilibrium crystallization or low-temperature hydrothermal models alone. In particular, the Raman-confirmed diamond spherules in emerald from Habachtal strengthen the interpretation that high-pressure mineral relics were introduced into the emerald-forming environment by supercritical media. A recurring feature of these occurrences is the presence of smooth, rounded, spherical, or subspherical inclusions, locally including composite textures such as spheres within spheres. These morphologies indicate mechanical abrasion, entrainment, and possible chemical modification during ascent. The high-pressure mineralogy and preservation of metastable phases require rapid transfer, fast enough to prevent complete inversion to lower-pressure polymorphs during emplacement. The most consistent explanation is movement by supercritical fluids or melts in which H_2O and aluminosilicate components are fully miscible. Such media combine high mobility with the capacity to carry dissolved elements and suspended mineral relics. In this model, supercritical fluids or melts can entrain tiny high-pressure crystals at depth, move them rapidly through the crust, and introduce them into mineral-forming environments that otherwise record much lower pressures. The Habachtal emerald, Waldheim prismatine granulite, Greifenstein topaz, and Variscan cassiterite examples also show that this mechanism is linked to element enrichment. Water-rich melt inclusions, Lorentzian element distributions, and exceptionally high Sn concentrations indicate non-equilibrium metal and volatile concentrations during the transition between supercritical and undercritical conditions. That provides a mechanism for selectively enriching elements such as Be and Sn and helps explain the unusually productive granitic and ore-forming systems. Overall, the evidence supports direct mantle–crust interaction mediated by supercritical fluids or melts. This process may be more widespread than previously recognized and should be considered when high-pressure mineral relics, rounded inclusion textures, water-rich melt inclusions, and extreme trace-element enrichments occur together in crustal rocks and mineral deposits.

Acknowledgment

I thank Paul Davidson (Hobart, Tasmania), Adolf Rericha (Falkensee, Germany), and Ulrich Recknagel (Schrobenhausen) for their discussions, which helped us prepare the underlying ACROFI lecture in 2022 in Nanjing.

References

1. Thomas R, Davidson P, Rericha A (2020) Emerald from the Habachtal: new observations. *Mineralogy and Petrology* 114: 161-172.
2. Thomas R, Davidson P, Rericha A, Veksler I (2021) Melt inclusions in emerald from the Habachtal/Austria after re-homogenization at 700°C and two kbar. *Academica Letters* 1-5.
3. Thomas R (2026b) Preliminary Raman evidence for boron-rich Al-B-C phases in natural topaz from Schneckenstein/Vogtland, Germany. Geol Earth Mar Sci 8.
4. Taleb NN (2018) Der schwarze Schwan - Die Macht höchst unwahrscheinlicher Ereignisse. *Pantheon*. PG: 624.
5. Thomas R, Davidson P, Rericha A, Voznyak DK (2022) Water-rich melt inclusions as "frozen "samples of the supercritical state in granites and pegmatites reveal extreme element enrichment resulting under non-equilibrium conditions. *Mineralogical Journal (Ukraine)* 44: 3-15.
6. Franz G, Grundmann G, Ackermand D (1986) Rock forming beryl from a regional metamorphic terrain (Tauern window, Austria): Paragenesis and crystal chemistry. *Tschermaks Miner Petrogr Mitt* 35: 167-192.
7. Grundmann G, Morteani G (1989) Emerald mineralization during regional metamorphism: the Habachtal (Austria) and Leydsdorp (Transvaal, South Africa) deposits. *Econ Geol* 84: 1835-1849.
8. Luckscheiter B, Morteani G (1980) Microthermometrical and chemical studies of fluid inclusions in minerals from Alpine veins from the penninic rocks of the central and western Tauern window (Austria/ltaly). *Lithos* 13: 61-77.
9. Ono S, Kikegawa T, Higi Y, Tange Y (2017) Precise determination of the phase boundary between coesite and stishovite in SiO_2. *Phys Earth Planet Int* 264: 1-6.
10. Rötzler J, Hagen B, Hoernes S (2008) Geothermometry of the ultrahigh-temperature Saxon granulites revised. Part I: New evidence from key mineral assemblage and reaction textures. *Eur J Mineral* 20: 1097-1115.
11. Kalkowsky E (1907) Der Korundgranulit von Waldheim in Sachsen. Abh. Naturwissenschaftlichen Gesellschaft ISIS Dresden 47-65.
12. Thomas R, Davidson P, Rericha A (2025) Zircon-reidite in prismatine granulite from Waldheim/Saxony. Chapter 11 in: Current Research Progress in Physical Science (ed. by Nagata) 156-162.
13. Thomas R (2026a) Origin of Sn in the Variscan tin deposit Ehrenfriedersdorf. *Geol Earth Mar Sci* 8: 1-8.
14. Thomas R (2024a) The $CaCl_2$-to rutile phase transition in SnO_2 from high to low pressure in nature. *Geol Earth Mar Sci* 6: 1-4.
15. Thomas R (2024b) Rhomboedric cassiterite as inclusions in tetragonal cassiterite from Slavkovský les - North Bohemia (Czech Republic). *Geol Earth Mar Sci* 6: 1-6.
16. Parakhonskiy G (2012) Synthesis and investigation of boron phases at high pressure and temperature. Dissertation, University of Bayreuth/Germany. Pg: 117.
17. Werheit H, Filipov V, Kuhlmann U, Schwarz U, Aermbrüster M, Leithe-Jasper U, Tanaka T, Higashi I, Lundström T, Gurin VN, Korsukova MM (2010) Raman effect in icosahedral boron-rich solids. *Sci Technol Adv Mater* 11: 1-27.

Citation:

Thomas R, Pei Ni (2026) Direct Mantle–Crust Interaction by Supercritical Fluids and Melts: Evidence from High-Pressure Mineral Inclusions. *Geol Earth Mar Sci* Volume 8(6): 1-7.